Monatsh Chem
DOI 10.1007/s00706-015-1499-3

ORIGINAL PAPER

An efficient selective oxidation of alcohols with iron zirconium phosphate under solvent-free conditions

Abdol Reza Hajipour[1,2] · **Hirbod Karimi**[2] · **Amir Masti**[2]

Received: 11 March 2015 / Accepted: 11 May 2015

Abstract Iron zirconium phosphate nanoparticles have been used as an efficient catalyst for the selective oxidation of a wide range of alcohols to their corresponding ketones or aldehydes using H_2O_2 as an oxidizing agent without any organic solvent or additive. The steric factors associated with the substrates had a significant influence on the reaction conditions. The results showed that this method can be applied for chemoselective oxidation of benzyl alcohols in the presence of aliphatic alcohols. The catalyst used in the current study was characterized by ICP-OES, XRD, N_2 adsorption–desorption, NH_3-TPD, Py-FTIR, SEM, and TEM.

Graphical abstract

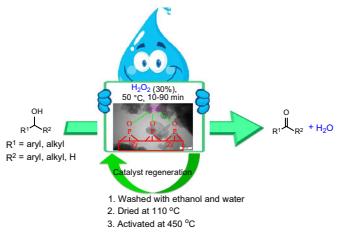

✉ Abdol Reza Hajipour
haji@cc.iut.ac.ir;
arhajipour@wisc.edu

[1] Department of Neuroscience, Medical School, Madison, University of Wisconsin, Madison, WI 53706-1532, USA

[2] Pharmaceutical Research Laboratory, Department of Chemistry, Isfahan University of Technology, Isfahan, IR, Iran

Keywords Iron zirconium phosphate · Heterogeneous catalysis · Solvent free · Nanoparticle · Alcohols

Introduction

α-Zirconium phosphate (ZP) is one of the most important compounds in inorganic chemistry, and the layered structure of this material has led to its use in a variety of different fields [1–3]. ZP behaves as a unique ion exchanger because of its exceptionally poor aqueous solubility, high thermal stability, resistance to radiation, and abrasive properties [4, 5]. The H^+ of the P–OH moiety in ZP can be exchanged for various other ions, resulting in an enlargement of the interlayer distance [6–10]. Several studies pertaining to the successful exchange of this proton with various divalent and trivalent cations have been presented in the literature [10–14]. It has also been reported that ZP possesses excellent selectivity towards Pb^{2+}, Zn^{2+}, and Fe^{3+} as an ion exchanger [15–17]. Furthermore, ZP has been reported to exhibit antibacterial activity when it was loaded with Cu^{2+}, Zn^{2+}, or Ce^{3+} [5, 12–14]. There have also been several reports concerning the catalytic activities of ion-exchanged materials of this type, including the use of zinc zirconium phosphate (ZPZn) and copper zirconium phosphate (ZPCu) as catalysts in the acetylation of alcohols and phenols and the use of potassium iron zirconium phosphate as a catalysts in Friedel–Crafts benzoylation reaction [9, 18–24].

The selective oxidation of alcohols into the corresponding carbonyl compounds is an important research field since the corresponding aldehyde, ketone, or carboxylic derivatives serve as important and versatile intermediates for the synthesis of various chemicals,

Published online: 02 June 2015

vitamins, drugs, and fragrances [25–27]. As a typical product of alcohol oxidation and a starting material, benzaldehyde (BzH) is an important chemical for the preparation of intermediates in the industry of dyestuff, agrochemicals, perfumery, and pharmaceuticals [27–29]. Thus, from economic and environmental viewpoints, there have been many recent publications emphasizing environmentally benign methods for the oxidation of alcohols, using molecular O_2 or aqueous H_2O_2 as the oxidant, in the presence and/or absence of the solvent such as $CuSO_4$ [25], $CuBr_2$ [26], AMPA [28], MPA/V_2O_5/Al_2O_3 [29], TEMPO-IL/CuCl [30], $Ni_3[Fe(CN)_6]_2$ [31], Pd/Fe@C [32], silicagel-TEMPO-NO_x [33], CoTM4PyP-MT [34], PdO/SBA-15 [35] (TEAH)$H_2PW_{12}O_{40}$ [36], Zn-Co-LDH [37], $RuCl_3{\cdot}3H_2O$ [38], VPO/HMS [39], AuRu/AC [40], oxidovanadium(V) complexes [41], Ag/SBA-15 [42], DHPDMDO [43], H_2WO_4/[C8mim][NTf_2] [44], SF-3-APTS-Fe(TClPP) [45], $NaBrO_3$/[bmim]Br [46], DCMBF [47], WO_4@PMO-IL [48], Cu-NHC-TEMPO complexes [49], Cu/AlO(OH) [50], SSA-SiO_2/$KMnO_4$ [51], copper/imidazolium/TEMPO [52], $Ca(ClO)_2$/Al_2O_3 [53], PVPTB [54], Au/UiO-66 [55], PSFC [56], Au/Al_2O_3 [57], PMo11 M (M = Co, Mn, Ni) [58], Mn(salen)OAc [59], BPFC [60], $KMnO_4$-aluminum silicate [61], KBr/oxone [62], PVP-H_2O_2 [63], TMP/$KMnO_4$ [64], $KMnO_4$-aluminum silicate [65], BQB [66], PS-TEMPO@Cu-IL [67], MPPC-alumina [68], $CuBr_2$/TEMPO/bipyridine [69], $KNa_4[Ag(HIO_6)_2]$ [70], CPCC/alumina [71], and Fe_3O_4/MPS/PIL [72]. Homogeneous catalysts have drawbacks in terms of their corrosive nature, pollution of the product with catalyst, tedious catalyst separation and post synthesis disposals, and recovery from the effluents. On the other hand, the design of a new catalyst which gives excellent conversion with maximum selectivity for organic transformation is one of the challenges in the field of catalysis. H_2O_2 is a green and very clean oxidant for liquid phase oxidations, because it provides a high content of active oxygen species and water is the only by-product. This oxidant is much cheaper and safer than most other organic and inorganic oxidants and it is also readily available. With growing environmental concerns, one of the most promising ways to achieve these goals seems to be the use of green and insoluble catalysts or of ecofriendly solvent-free conditions. When an insoluble catalyst is used, it can be easily recovered from the reaction mixture by simple filtration and recycled and can be reused several times, making the process more economically and environmentally viable. Furthermore, the reported examples have demonstrated that heterogeneous catalysts typically require easier work-up procedures. With this in mind, and as part of ongoing work towards the development of efficient green catalysts for organic transformations [73, 74] with particular emphasis on the oxidation of alcohols [23], we report herein the use of iron zirconium phosphate (ZPFe) as an efficient catalyst for the mild and convenient selective oxidation of alcohols which was characterized by ICP-OES, XRD, BET, NH_3-TPD, Py-FTIR, SEM, and TEM.

Results and discussion

Characterization

The ICP-OES analyses of ZP and ZPFe are shown in Table 1. The results obtained in the current study for ZPFe were compared with those reported previously in the literature [8–10]. Our results revealed that there was a negligible leach of iron ions into the reaction media after the reaction (i.e., following the first use of the catalyst).

Figure 1 shows the powder XRD patterns of the ZP and ZPFe materials. The results show some characteristic reflections in the 2θ range of 5°–40°. The diffraction peak in ZP at 2θ–12° was assigned to a d_{002} basal spacing of 7.5 Å between the planes, which was consistent with the patterns previously reported for ZP and its derivatives with a hexagonal crystal system [2]. It shows that the d-spacing of the (002) plane of ZPFe had increased, which indicated that the Fe^{3+} ions had intercalated into the interlayer of ZP and increased the d_{002} basal interlamellar spacing of ZP from 7.5 to 9.3 Å. It is well known that the ion radii of Fe^{3+} (0.64 Å) and hydrated Fe^{3+} (3.9 Å) are smaller than the basal spacing of ZP (7.5 Å) [75, 76]. These results therefore indicated that Fe^{3+} ions had inserted into the interlayer of ZP and increased the basal spacing of the modified ZP after the exchange [4, 9, 10, 17]. Taken together, these data indicated that ZPFe had been formed successfully. The XRD pattern of the ZPFe catalyst after the 8th run showed that the basal spacing of ZP was about 10.5 Å, which was only a little larger than that of the fresh ZPFe catalyst. This increase may have occurred because of the presence of less Fe^{3+} on the surface of ZP, and an increase in the number of water molecules between the layers following the seventh run (i.e., Fe^{3+} ions may have been washed off during the regeneration of the catalyst, Table 1).

Figure 2 shows the N_2 adsorption–desorption isotherm of ZPFe, as a representative example, in the relative pressure range (p/p_0) of 0.1–1.0. The surface area of ZPFe was determined to be 120.5 m^2/g. The isotherm for ZPFe shows three adsorption stages. The first of these stages was observed at $p/p_0 < 0.36$, whereas the second stage was observed in the range of $0.36 < p/p_0 < 0.92$, and the third stage was observed at higher relative pressures ($p/p_0 > 0.92$). The N_2 adsorption–desorption isotherm of ZPFe exhibited a typical type IV isotherm shape with a distinct hysteresis loop, which is characteristic of a mesoporous material [77]. The hysteresis loop (type H3) is

Table 1 Element contents of ZPFe (atom%) and physical properties of the catalysts before and after reaction

Sample	Fe	O	Zr	P	BET/m^2 g^{-1}	Total acidity/mmol NH_3 g^{-1}
ZP	–	63.1	13.6	23.3	128.7	2.7
ZPFe	9.1	59.3	11.9	19.7	120.5	1.9
ZPFe[a]	9.0	59.6	11.8	19.6	119.7	1.76
ZPFe[b]	2.8	63.6	13.8	19.8	64.2	0.48

[a] After the first cycle

[b] After the 8th cycle

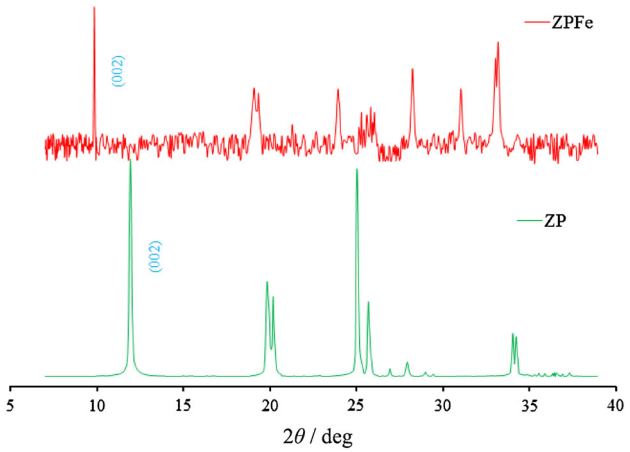

Fig. 1 XRD patterns of powder ZP (down), ZPFe (up)

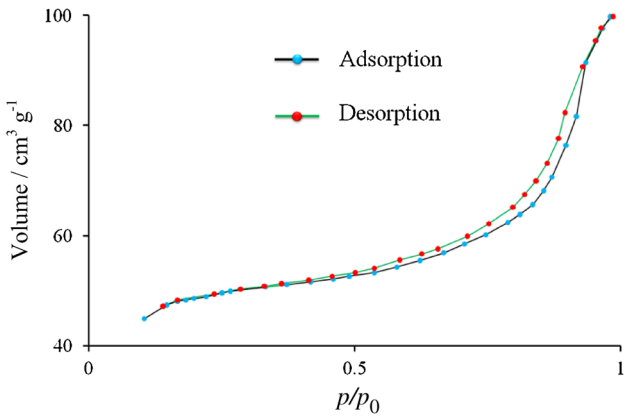

Fig. 2 N_2 adsorption–desorption isotherm of ZPFe

associated with the occurrence of capillary condensation in the mesopores, which indicates the presence of a mesoporous structure in the ZPFe catalyst. The observed increase in adsorption at the higher p/p_0 value indicated the presence of larger mesopores in the sample [9, 10]. The surface area of ZPFe after the 8th run was found to be 64.2 m^2/g.

Pyridine adsorption was used to determine the acidic sites using FTIR. Prior to the measurements, 20 mg of a catalyst was pressed in self-supporting disc and activated in

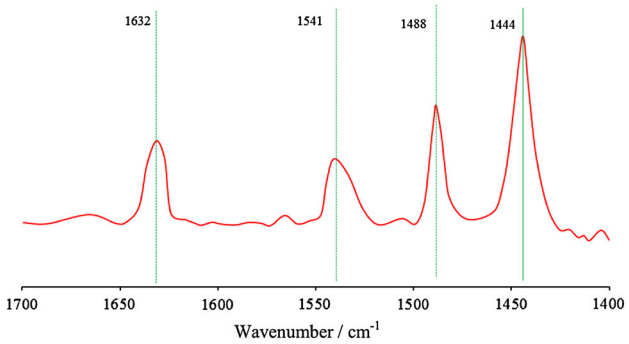

Fig. 3 Pyridine-desorbed FTIR spectra of the calcined ZPFe

the IR cell attached to a vacuum line at 350 °C for 4 h. The adsorption of pyridine was performed at 150 °C for 30 min. The excess of probe molecules was further evacuated at 150 °C for 0.5 h. The adsorption–evacuation was repeated several times until no changes in the spectra were observed (Fig. 3). The main bands observed over the samples are assigned according to the literature data [78, 79]. Pyridine-desorbed FTIR spectra of the ZPFe show the strong bands at 1632 and 1541 cm^{-1}, indicating typical pyridinium ion. The band at 1488 cm^{-1} is a combination band between those at 1541 and 1444 cm^{-1}, corresponding to Brønsted and Lewis acid sites, respectively [9, 10].

Total acidity of the samples was determined by temperature-programmed desorption of ammonia (TPD-NH_3) with a Quantachrome ChemBET 3000. Before the adsorption of ammonia, the samples were pre-treated in He at 250 °C for 30 min and then, 1 h at 350 °C and cooled to 100 °C. Then, ammonia was adsorbed on the samples for 1 h. The TPD-NH_3 was carried out between 150 and 550 °C, at 10 °C/min, and analyzed by a thermal conductivity detector (TCD) for continuous monitoring of the desorbed ammonia. TPD-NH_3 provides a quantitative estimation of the total number of acid sites and the distribution of acid strengths. Because of the strong basicity of NH_3 gas, it was expected that all acid sites on the catalysts interact with NH_3. The total amount of NH_3 desorbed after saturation permits the quantification of the number of acid sites on the surface, while the position of the peak, desorption temperature, indicates the strength of

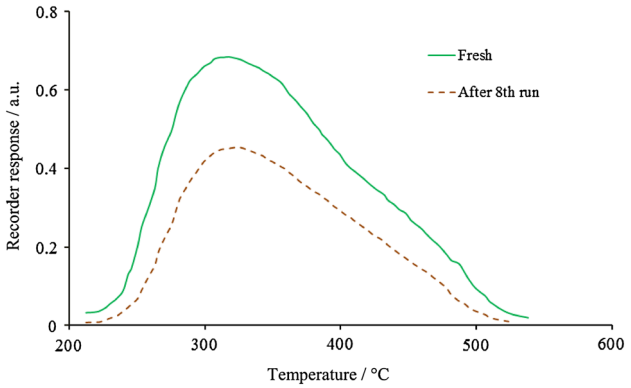

Fig. 4 NH_3-TPD profile of ZPFe

the catalyst, i.e., the higher temperature of desorption, the stronger the acid strength [73]. The TPD-NH_3 curves of ZPFe are shown in Fig. 4. ZPFe desorbed ammonia in a wide range of temperatures from 212 to 538 °C, which mostly corresponds to the medium and the strong acidic sites. The NH_3 desorption peak at temperatures below 250 °C belongs to the physisorption/chemisorptions of NH_3 molecules on weak acidic sites. The peak at about 250–450 °C shows the existence of intermediate strength acidic sites and finally the peak at 450–538 °C demonstrates the presence of strong acidic sites on the surface of ZPFe. Figure 4 shows that the desorption of ammonia starts at almost 212 °C, centered at 317. The NH_3-TPD curves subsequently decreased with further increase in temperature and almost complete at 538 °C.

This indicates that ZPFe contains a considerable number of acid sites which is attributed to the presence of Fe^{3+} groups on the surface of zirconium phosphate layers and makes it suitable as a solid acid catalyst. The extent of desorptions is found to be ca. 1.9 mmol NH_3/g of catalyst. A TPD experiment was carried out after the 8th cycle by recovering the catalyst, to magnify the difference from the fresh catalysts (Table 1).

The SEM image of ZP (Fig. 5a) revealed the presence of hexagonal plates with well-defined shapes and very smooth surfaces. Figure 5b, c shows the SEM images of ZPFe. These images revealed that the structure of ZPFe was much less ordered than that of ZP, and that the ZPFe particles had aggregated to form both sheets and spheres of different shapes and sizes [4, 10].

Figure 6 shows the TEM images of ZPFe. It shows that ZPFe catalyst retained the original morphology of ZP (layered structure) and that the particles were approximately 150 nm in size. These images also showed nanoparticles of different sizes on the smooth surface of the ZP.

The presence of metallic crystal nanoparticles on the surface of ZP indicated that the iron deposited on the surface of the ZP had agglomerated. Similar observations have also been reported for zinc and cerium with ZP [12, 14, 24]. Figures 5d and 6c show the SEM and TEM images of the catalyst following its 8th run, respectively. Both of these images showed that the sheets and particles had conglomerated to a much greater extent following the 8th run because of the process used to regenerate the catalyst.

Oxidation reaction and expected mechanism

Initially, the benzyl alcohol (BzOH) was selected as the model substrate to determine the optimal conditions and the results are summarized in Table 2. Although the major product was BzH, benzoic acid was also formed as a side product (Table 2, entries 4, 5, 8, 11, 14, 15). It was found that by changing the reaction parameters such as time (Table 2, entries 1–5), mole ratio (Table 2, entries 6–8), temperature (Table 2, entries 9–11) or catalyst mol % (Table 2, entries 12–15), the selectivity and/or yield were changed.

As can be seen from Table 2, an increase in the reaction time (up to 15 min) causes an increase in yield of BzH as the only product but after that, benzoic acid was produced as a by-product and BzH yield was reduced to 65 %. When the mole ratio of BzOH: H_2O_2 reached at 1:3, highest yield was obtained and then, by further increasing of BzOH: H_2O_2 mol ratio, the yield was slightly increased, but selectivity toward BzH decreased sharply (Table 2, entries 2, 6–8). For finding the optimum reaction temperature for oxidation of BzOH, the reaction was performed at different temperatures. The yield of BzH was very low at room temperature even after 90 min (Table 2, entry 9). Table 2 shows that the temperature rising can accelerate the reaction (up to 50 °C), but increasing the temperature further results in a decrease in the yield, which might be due to the overoxidation of BzH to benzoic acid or self-decomposition of H_2O_2 at higher temperatures, leading to insufficient oxidation of BzOH (entries 2, 9–11). Hence, when the reaction was performed at 50 °C, BzOH: H_2O_2 mol ratio 1:3 and 15 min, best result was achieved (Table 2, entry 2). To evaluate the role of our catalyst, the oxidation reaction was performed when the ZP was used as the catalyst (Table 2, entry 17). Also, the oxidation reaction was performed in the absence of the any catalyst (Table 2, entry 16). No significant amount of BzH was detected indicating that H_2O_2 alone is unable to oxidize BzOH to BzH.

As shown in Table 3, a wide range of alcohols bearing either electron-donating or electron-drawing groups were successfully oxidized into their corresponding carbonyl compounds within short reaction times. Notably, the efficient transformations of primary alcohols into the desired aldehydes were observed without any overoxidation to the corresponding carboxylic acid (Table 3, entries 1–14). Both electron-donating and electron-drawing groups

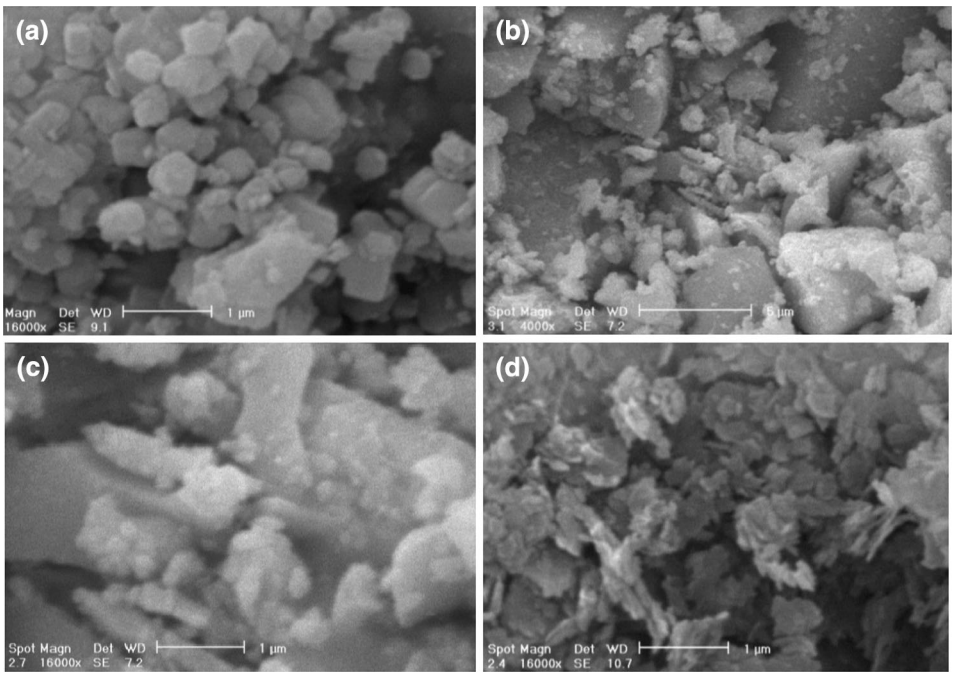

Fig. 5 SEM images of regular morphology of prepared ZP (**a**), ZPFe fresh (**b**, **c**) and after 8th run (**d**)

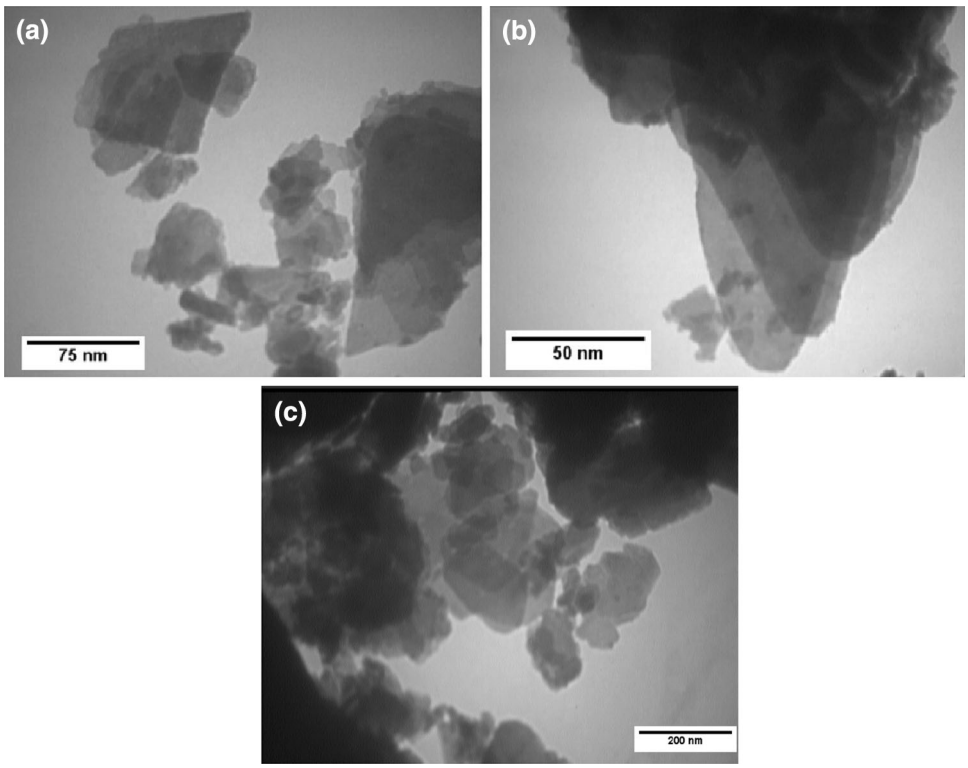

Fig. 6 TEM images of regular morphology of prepared ZPFe fresh (**a**, **b**) (different magnification) and after the 8th run (**c**)

accelerated the oxidation reaction, but *ortho*-substituted substrates (Table 3, entries 2, 5, 7, 9) gave relatively lower yields compared to the corresponding *para*-isomer due to steric hindrance [26, 50, 52]. Compared to benzylic alcohols, aliphatic alcohols showed relatively low reactivity toward oxidation (Table 3, entries 22–25). It should be noted that under this reaction condition, various secondary alcohols were oxidized into their corresponding ketone in fair yields (Table 3, entries 15–21, 23, 25). To investigate the selectivity of this method, a mixture of 1-hexanol and BzOH was subjected to oxidation, BzH was produced in 85 % yield and only 5 % of 1-hexanal was detected. Such selectivity can be considered as a useful practical achievement in oxidation of alcohols.

Table 2 Oxidation conditions of benzyl alcohol (BzOH)

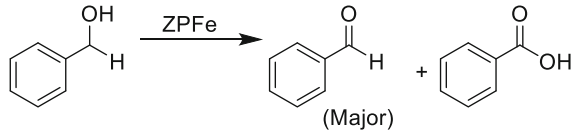

Entry	Time/min	Mole ratio[a]	Temp./°C	Catalyst/mol%	Yield[b]/%	Selectivity[c]/%
1	5	1:3	50	0.5	58	>99
2	10	1:3	50	0.5	69	>99
3	15	1:3	50	0.5	90	>99
4	20	1:3	50	0.5	82 (89)	65 (35)
5	25	1:3	50	0.5	75 (91)	60 (40)
6	15	1:1	50	0.5	55	>99
7	15	1:2	50	0.5	73	>99
8	15	1:4	50	0.5	91 (91)	77 (23)
9	90	1:3	r.t	0.5	25	>99
10	90	1:3	40	0.5	72	>99
11	15	1:3	60	0.5	84 (87)	70 (30)
12	15	1:3	50	0.1	50	>99
13	15	1:3	50	0.25	60	>99
14	15	1:3	50	0.75	80 (82)	75 (25)
15	15	1:3	50	1.0	75 (88)	65 (35)
16	120	1:3	50	–	–	–
17[d]	120	1:3	50	0.5	5	>99

[a] BzOH: H_2O_2 mol ratio

[b] Isolated yield for BzH (benzoic acid as the main by-product)

[c] Selectivity for BzH (benzoic acid as the main by-product)

[d] ZP was used as the catalyst (blank)

Based on the observation, the typical mechanism proposed for ZPFe-catalyzed oxidation of alcohols with H_2O_2 is given in Scheme 1. At first, the Fe Lewis acid site (on the surface of ZPFe) interacts with H_2O_2 to form (I) and it reacts with alcohol to give an intermediate (II) which gives the corresponding carbonyl compound and regenerated active sites by two steps of dehydration. Hence, any steric hindrance around hydroxyl group of alcohols such as presence of substitutes at the *ortho* position (Table 3, entries 2, 5, 7, 9) or more hindered secondary alcohols (Table 3, entries 15–21) causes longer reaction time and lower yields. Almost similar behavior was reported before [26, 50, 52].

The reusability of the ZPFe catalyst was investigated under the optimum reaction conditions for the oxidation of alcohols, and the results are shown in Table 4. The elemental composition of the catalyst remained largely unchanged following its 8th run, although the amount of iron in the catalyst was reduced by almost 75 % compared with the first run (Table 1). The recycled ZPFe catalyst gave a similar product yield to the freshly prepared catalyst up until the sixth cycle. All products were identified by their GC–MS (GC-Mass, Agilent 5975C) and ^{1}H NMR spectra (Bruker-Avance AQS 400 MHz spectrometer; in $CDCl_3$) with authentic samples [23, 28, 47, 49, 51].

A comparison of the catalytic efficiency of ZPFe with selected previously known catalysts is collected in Table 5. BzOH was oxidized to BzH in less than 15 min at 50 °C in 90 % isolated yield using the present protocol (Table 5, entry 17). Of course, the reaction conditions are different, but the catalyst used in this study (ZPFe) might be one of the best catalysts with regard to lower reaction time and temperature, better BzH yield and selectivity toward BzH as the major product. The catalysts can also be easily regenerated for further applications.

Conclusion

In summary, we have reported the catalytic performance of water-insoluble ZPFe in the oxidation of alcohols using H_2O_2. The catalyst was characterized by various methods

Table 3 The oxidation reaction in the presence of ZPFe

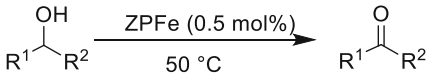

Entry	R^1	R^2	Time/min	Mole ratio[a]	Yield[b]/%	Selectivity/%
1	Ph	H	15	1:3	90	>99
2	2-MeO–C_6H_4	H	10	1:3	83	>99
3	4-MeO–C_6H_4	H	10	1:3	95	>99
4	4-Me–C_6H_4	H	10	1:3	90	>99
5	2-Cl–C_6H_4	H	10	1:3	88	>99
6	4-Cl–C_6H_4	H	10	1:3	95	>99
7	2-Br–C_6H_4	H	10	1:3	81	>99
8	4-Br–C_6H_4	H	10	1:3	95	>99
9	2-NO_2–C_6H_4	H	10	1:3	88	>99
10	4-NO_2–C_6H_4	H	10	1:3	95	>99
11	4-NC–C_6H_4	H	10	1:3	95	>99
12	Furfuryl alcohol	–	10	1:3	90	>99
13	2-Naphthyl	H	10	1:3	92	>99
14	PhCH=CH	H	10	1:3	91	>99
15	Ph	Ph	60	1:3	80	>99
16	Ph	CH_3	60	1:3	85	>99
17	4-MeO–C_6H_4	CH_3	45	1:3	88	>99
18	4-Me–C_6H_4	CH_3	45	1:3	85	>99
19	4-Cl–C_6H_4	CH_3	45	1:3	87	>99
20	4-Br–C_6H_4	CH_3	45	1:3	88	>99
21	4-NO_2–C_6H_4	CH_3	45	1:3	92	>99
22	$CH_3CH_2CH_2$	H	90	1:4	81	>99
23	CH_3CH_2	CH_3	90	1:4	70	>99
24	$CH_3(CH_2)_4$	H	90	1:4	80	>99
25	Cyclohexanol	–	90	1:4	72	>99
26[c]	Ph	H	20	1:3	85	>99
	$CH_3(CH_2)_4$	H	20	1:3	5	>99

[a] Substrate: H_2O_2 mol ratio

[b] Isolated yield. All products were identified by their GC–MS and ^{1}H NMR spectra with authentic samples [23, 28, 47, 49, 51]

[c] Reaction conditions: BzOH (5 mmol), 1-hexanol (5 mmol), H_2O_2 (0.015 mol)

and results showed good agreement with the literature. ZPFe showed outstanding catalytic performance with excellent conversion of BzOH and selectivity to BzH at 50 °C for 15 min. The selectivity remained unchanged for all the reactions, although the yields were found to be affected by the steric hindrance. Alcohols having bulky groups required a longer reaction time compared with others. The results clearly reveal that this method can be applied for chemoselective oxidation of BzOHs in the presence of aliphatic alcohols. This procedure is environmentally benign, general, efficient, high yielding, safe, and operationally simple.

Experimental

All chemicals and solvents were purchased from Sigma-Aldrich and Merck Chemical Companies and used without further purification. The chemical composition of the ZPFe catalyst was evaluated at different stages of the reaction (i.e., before and after the catalytic reaction) by ICP-OES using an Optima 7300 V ICP-OES spectrometer (PerkinElmer). The samples were ground into a fine powder and analyzed by XRD on a Philips X'pert X-ray diffractometer. The specific surface areas of the samples were determined from their N_2 adsorption–desorption isotherms using the

Scheme 1

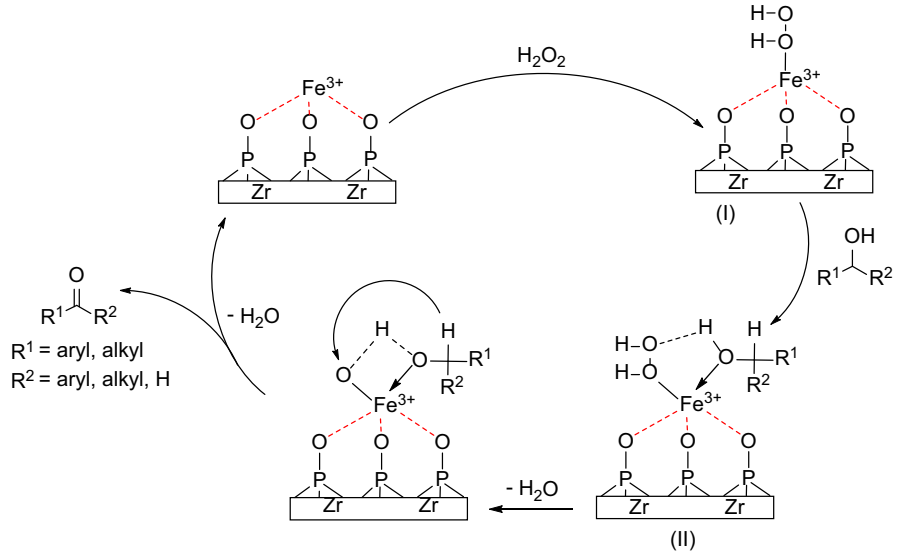

Table 4 The catalyst re-used under the optimum reaction conditions for acetylation of phenol

Substrate[a]	Fresh	Run 1	Run 2	Run 3	Run 4	Run 5	Run 6	Run 7	Run 8
BzOH	90	90	90	90	87	87	86	84	67

[a] Reaction conditions: BzOH (5 mmol), H_2O_2 (0.015 mol), catalyst (0.5 mol %), 50 °C, 15 min

Brunauer–Emmett–Teller (BET) method on a Quantachrome ChemBET 3000 instrument. Each sample was degassed at 400 °C for 2 h before being analyzed to remove any adsorbed species from their surfaces. The BET surface areas of the materials were estimated from their N_2 adsorption–desorption isotherms. The surface morphologies of the ZP and ZPFe materials were studied by SEM on a Philips XL scabbing electron microscope (Philips). TEM images of ZPFe were obtained on a CENTRA 100 TEM system (Zeiss). All yields refer to isolated products after purification. All products were characterized by comparison with authentic samples and by spectroscopy data FT-IR and ^{1}H NMR analysis. ^{1}H NMR spectra were recorded on a Bruker-Avance AQS 400 MHz spectrometer. The spectra were measured in $CDCl_3$ unless otherwise stated, relative to TMS (0.00 ppm). FT-IR spectra were recorded on a Jasco-680 spectrophotometer.

Catalyst synthesis

All of the reagents and solvents used in the current study were purchased from Merck Chemical Company and used without further purification. The catalyst was prepared according to previously published procedures, with minor modifications [2, 8–10]. ZP was prepared according to the following procedure. $ZrOCl_2{\cdot}8H_2O$ (5 g) was heated at reflux in a solution of 50 cm^3 H_3PO_4 (12 mol/dm^3) for 24 h. The resulting mixture was cooled to ambient temperature to give a suspension, which was filtered, and the filter cake was then washed with a solution of H_3PO_4 (0.1 mol/dm^3) until the filtrate was free of chloride ions. The filter cake was then washed several times with distilled water until the pH of the filtrate was neutral. The solid was then collected and dried in an oven at 110 °C for 24 h [2]. ZPFe was prepared through an ion exchange reaction [8–10]. Briefly, 3 g ZP was dispersed in 50 cm^3 deionized water at 50 °C, and the resulting suspension was treated with 100 cm^3 of a solution of $Fe(OAc)_3$ (0.1 mol/dm^3) in water (excess amount of Fe^{3+}). This mixture was then heated at reflux for 4 d. It is noteworthy that the acetate ion performed effectively as a base to keep the hydrogen ion concentration in solution sufficiently low to achieve high loadings of the catalyst [8]. A complete exchange between the cations and the hydrogen ions of the P–OH groups could not be achieved in less than 3 d or at temperatures below 80 °C [13]. The resulting slurry was filtered hot to

Table 5 Comparison of protocols for the oxidation of benzyl alcohol

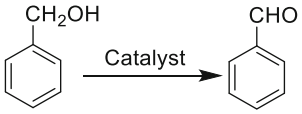

Entry	Catalyst	*T*/°C	Time/min	BzOH:H_2O_2[a]	Yield/%	Selectivity[b]/%	References
1	$CuSO_4$	100	15	1:3	69	71	[25]
2	$ZnBr_2$	Reflux	90	1:1[c,d]	96	100	[27]
3	TEMPO-IL/CuCl	40	720	–[e]	55	100	[30]
4	$Ni_3[Fe(CN)_6]_2$	75	240	1:3	36[f]	100	[31]
5	$Zn_4(P_2W_{15}O_{56})^{16-}$	Reflux	45	1:10[d]	94	100	[35]
6	$(TEAH)H_2PW_{12}O_{40}$	100	180	1:0.8	99.6[f]	100	[36]
7	Zn-Co-LHD	65	540	1:5[d,g]	72[f]	90	[37]
8	$H_4SiW_{12}O_{40}/SiO_2$	r.t.	240	–[e]	82[d]	100	[39]
9	SF-3-APTS–Fe(TClPP)	r.t.	180	1:1[d,g]	99	100	[45]
10	WO_4@PMO-IL	90	720	1:5[d]	75[f]	100	[48]
11	Au/UiO-66	80	1200	–[e]	63.7	100	[55]
12	PSFC	r.t.	7	1:5[d]	93	100	[56]
13	Au/Al_2O_3	100	15	–[e,h]	45[f]	86	[57]
14	$PMo_{11}Co$	90	1440	1:3	56.5[f]	90.9	[58]
15	Mn(salen)OAc	r.t.	30	1:2[d,i]	91	100	[59]
16	BPFC	70	5	1:1.5	95	100	[60]
17	ZPFe	50	15	1:3	90	>99	This work

[a] Mole ratio

[b] Selectivity for BzH

[c] Chloramine-T as the oxidant

[d] CH_3CN as solvent

[e] O_2 atmosphere as the oxidant

[f] Conversion of BzOH

[g] TBHP as the oxidant

[h] Toluene as solvent

[i] $NaIO_4$ as the oxidant

Scheme 2

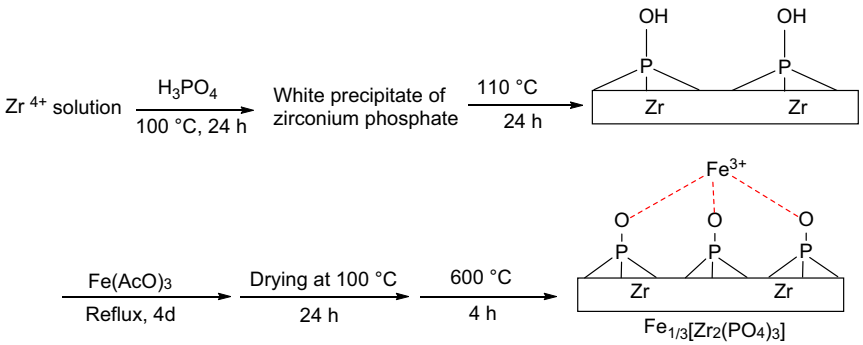

give a light yellow solid, which was washed with distilled water until no Fe^{3+} ions could be detected in the filtrate (i.e., until the filtrate was colorless). The solid product was then dried at 100 °C for 24 h before being calcined at 600 °C for 4 h to give the final product, $Fe_{1/3}[Zr_2(PO_4)_3]$, as a pale yellow solid (Scheme 2).

General experimental procedure for the oxidation reaction

Substrate (5 mmol) and ZPFe (0.5 mol %) were added into a 25 cm^3 two-necked flask. It was heated in an oil bath to 50 °C and then, 30 % H_2O_2 (0.015 mol) was added slowly with continuous stirring for the specified time. The reaction progress was monitored by GC. At the end, the reaction mixture was cooled to room temperature and then, the catalyst was removed from the reaction mixture by centrifuge. After that, the organic layer was separated from the aqueous phase by extraction with *n*-hexane and dried over anhydrous $CaCl_2$. The identity of reaction products was confirmed by FT-IR, GC–MS, and ^1H NMR.

Recyclability studies of catalyst

To examine the recyclability of the catalyst, the used ZPFe was recovered from the reaction media and re-used. For recycling, after the first use, the catalyst was separated from the reaction mixture by centrifugation, washed sequentially with ethanol and water before being dried at 110 °C for 2 h, and then activated at 450 °C for 2 h.

Acknowledgments We gratefully acknowledge the funding support received for this project from the Isfahan University of Technology (IUT), IR, Iran.

References

1. Gan H, Zhao X, Song B, Guo L, Zhang R, Chen C, Chen J, Zhu W, Hou Z (2014) Chin J Catal 35:1148
2. Sun L, Boo WJ, Sue HJ, Clearfield A (2007) New J Chem 31:39
3. Hajipour AR, Karimi H (2014) Mater Lett 116:356
4. Sun Z, Liu Z, Xu L, Yang Y, He Y (2004) Stud Surf Sci Catal 154:1060
5. Shi QS, Tan SZ, Ouyang YS, Yang QH, Chen AM, Li WR, Shu XL, Feng J, Feng J, Chen YB (2011) Adv Mater Res 150:852
6. Khare S, Chokhare R (2012) J Mol Catal A: Chem 353–354:138
7. Wang Q, Yu J, Liu J, Guo Z, Umar A, Sun L (2013) Sci Adv Mater 5:469
8. Clearfield A, Kalnins JM (1978) J Inorg Nucl Chem 40:1933
9. Gawande M, Deshpande S, Sonavane S, Jayaram R (2005) J Mol Catal A: Chem 241:151
10. Khare S, Chokhare R (2011) J Mol Catal A: Chem 344:83
11. Giannoccaro P, Gargano M, Fanizzi A, Ferragina C, Aresta M (2005) Appl Catal A 284:77
12. Cai X, Dai G-J, Tan S-Z, Ouyang Y, Ouyang Y-S, Shi Q-S (2012) Mater Lett 67:199
13. Yang Y, Dai G, Tan S, Liu Y, Shi Q, Ouyang Y (2011) J Rare Earths 29:308
14. Dai G, Yu A, Cai X, Shi Q, Ouyang Y, Tan S (2012) J Rare Earths 30:820
15. Zhang QR, Du W, Pan BC, Pan BJ, Zhang WM, Zhang QJ, Xu ZW, Zhang QX (2008) J Hazard Mater 152:469
16. Costantino U, Szirtes L, Kuzmann E, Megyeri J, Lázár K (2001) Solid State Ionics 141–142:359
17. Gobechiya ER, Kabalov YK, Orlova AI, Trubach IG, Bykov DM, Kurazhkovskaya VS (2004) Crystallogr Rep 49:390
18. Wang XY, Hua WM, Yue YH, Gao Z (2013) Chem J Chin Univ 34:1913
19. Barhon Z, Saffaj N, Albizane A, Azzi M, Mamouni R, El Haddad M (2012) J Mater Environ Sci 3:879
20. Pylinina A, Mikhalenko I (2013) Russ J Phys Chem 87:372
21. Pylinina A, Mikhalenko I (2011) Russ J Phys Chem 85:2109
22. Hajipour A, Karimi H, Karimzadeh M (2014) Monatsh Chem 145:1461
23. Hajipour AR, Karimi H (2014) Chin J Catal 35:1529
24. Hajipour AR, Karimi H (2014) Chin J Catal 35:1982
25. Ahmad JU, Räisänen MT, Leskelä M, Repo T (2012) Appl Catal A 411–412:180
26. Hu Z, Kerton FM (2012) Appl Catal A 413–414:332
27. Wang P, Cai J, Yang J, Sun C, Li L, Hu H, Ji M (2013) Tetrahedron Lett 54:533
28. Hosseinzadeh R, Tajbakhsh M, Khaledi H (2008) J Chin Chem Soc 55:239
29. Rao PSN, Rao KTV, Sai Prasad PS, Lingaiah N (2011) Chin J Catal 32:1719
30. Liu L, Ji LY, Wei YY (2008) Monatsh Chem 139:901
31. Ali SR, Chandra P, Latwal M, Jain SK, Bansal VK, Singh SP (2011) Chin J Catal 32:1844
32. Zhang H, Liu Y, Zhang X (2011) Chin J Catal 32:1693
33. Zhang H, Fu L, Zhong H (2013) Chin J Catal 34:1848
34. Zhou X, Ji H (2012) Chin J Catal 33:1906
35. Atashin H, Malakooti R (2014) J Chin Chem Soc 61:1039
36. Su H, Yang C (2014) Chin J Catal 35:1224
37. Zou X, Goswami A, Asefa T (2013) J Am Chem Soc 135:17242
38. Zhou C, Liu Y (2010) Chin J Catal 31:656
39. Mahdavi V, Hasheminasab HR, Abdollahi S (2010) J Chin Chem Soc 57:189
40. Villa A, E-chan-thaw C, Schiavoni M, Campisi S, Wang D, Prati L (2014) Chin J Catal 35:945
41. Ghorbani-Vaghei R, Veisi H, Amiri M (2007) J Chin Chem Soc 54:1257
42. Ma L, Jia L, Guo X, Xiang L (2014) Chin J Catal 35:108
43. Azarifar D, Najminejad Z, Khosravi K (2013) J Iran Chem Soc 10:979
44. Chatel G, Monnier C, Kardos N, Voiron C, Andrioletti B, Draye M (2014) Appl Catal A 478:157
45. Rahimi R, Ghoreishi SZ, Dekamin MG (2012) Monatsh Chem 143:1031
46. Shaabani A, Farhangi E, Rahmati A (2008) Monatsh Chem 139:905
47. Khazaei A, Raiatzadeh A, Rostami A (2007) J Chin Chem Soc 54:465
48. Karimi B, Rostami FB, Khorasani M, Elhamifar D, Vali H (2014) Tetrahedron 6114
49. Liu X, Xia Q, Zhang Y, Chen C, Chen W (2013) J Org Chem 78:8531
50. Babu SG, Priyadarsini PA, Karvembu R (2011) Appl Catal A 392:218
51. Mirjalili BF, Zolfigol MA, Bamoniri A, Zarei A (2004) J Chin Chem Soc 51:509
52. Chen C, Liu B, Chen W (2013) Synthesis 45:3387
53. Mojtahedi MM, Saidi MR, Bolourtchian M, Shirzi JS (2001) Monatsh Chem 132:655

54. Ali Zolfigol M, Hajjami M, Ghorbani-Choghamarani A (2012) J Iran Chem Soc 9:13
55. Zhu J, Wang PC, Lu M (2014) Appl Catal A 477:125
56. Bekhradnia AR, Zahir F, Arshadi S (2008) Monatsh Chem 139:521
57. Rautiainen S, Simakova O, Guo H, Leino AR, Kordás K, Murzin D, Leskelä M, Repo T (2014) Appl Catal A 485:202
58. Pathan S, Patel A (2013) Appl Catal A 459:59
59. Bahramian B, Mirkhani V, Moghadam M, Amin AH (2006) Appl Catal A 315:52
60. Özgün B, Yaylaoglu A, Şendil K (2007) Monatsh Chem 138:161
61. Lou JD, Gao CL, Li L, Fang ZG (2006) Monatsh Chem 137:1071
62. Moriyama K, Takemura M, Togo H (2014) J Org Chem 79:6094
63. Ghorbani-Choghamarani A, Azadi G (2011) J Iran Chem Soc 8:1082
64. Zhu C, Ji L, Wei Y (2010) Monatsh Chem 141:327
65. Lou J-D, Zhu L-Y, Wang L-Z (2004) Monatsh Chem 135:31
66. Laila A (2013) Monatsh Chem 144:307
67. Liu L, Liu D, Xia Z, Gao J, Zhang T, Ma J, Zhang D, Tong Z (2013) Monatsh Chem 144:251
68. Tajbakhsh M, Ghaemi M, Sarabi S, Ghassemzadeh M, Heravi MM (2000) Monatsh Chem 131:1213
69. Geißlmeir D, Jary WG, Falk H (2005) Monatsh Chem 136:1591
70. Bugarčić Z, Novokmet S, Senić Z, Bugarčić Z (2000) Monatsh Chem 131:799
71. Heravi MM, Kiakoojori R, Mirza-Aghayan M, Tabar-Hydar K, Bolourtchian M (1999) Monatsh Chem 130:481
72. Zhu J, Wang PC, Lu M (2013) Monatsh Chem 144:1671
73. Hajipour AR, Karimi H (2014) Appl Catal A 482:99
74. Hajipour AR, Karimi H (2014) Chin J Catal 35:1136
75. Bingham PA, Hannant OM, Reeves-Mclaren N, Stennett MC, Hand RJ (2014) J Non-Cryst Solids 387:47
76. Pandit AA, Shitre AR, Shengule DR, Jadhav KM (2005) J Mater Sci 40:423
77. Sing KS (1985) Pure Appl Chem 57:603
78. Corma A (1995) Chem Rev 95:559
79. Tyagi B, Chudasama CD, Jasra RV (2006) Appl Clay Sci 31:16